Journal of Applied Sciences Research, 5(1): 57-65, 2009

Experimental Investigation of Abutment Scour in Sandy Soil

[1]M.M. Abou-Seida, [2]G.H.Elsaeed, [1]T.M.S. Mostafa, [2]E.F.M. Elzahry

[1]Irrigation and Hydraulics Department, Faculty of Engineering, Cairo University, Giza, Egypt.
[2]Civil Engineering Department, Faculty of Engineering (Shoubra), Benha University, Egypt.

Abstract: Local scour around bridge abutments in alluvial channels is an unavoidable problem. Accurate prediction of the scour hole depth and pattern is essential for a safe and economic design of bridge foundation. The local scour pattern around bridge abutments depends on the abutment shape, local flow field and type and properties of the erodible bed material. The current experimental study is carried out to investigate the local scour around vertical bridge abutments in sandy soils and to estimate the local scour pattern formed around the bridge abutment at equilibrium condition. In the laboratorial experimentations of the present study vertical wall abutment is used with three different sizes. Twenty four laboratorial experiments are carried out with flow parameters achieving clear water scour conditions using sandy soil as erodible medium. From the experimental results, empirical formulas are developed for sandy soil to predict the equilibrium scour pattern around vertical bridge abutment (equilibrium scour depth and scour width) in terms of the dominating factors that affect and control scour process (Froude number and vertical-wall abutments dimensions).

Key words: Abutment, non cohesive sand, clear water scour, scour pattern.

INTRODUCTION

The protrusion of a bridge abutment into the main channel or the floodplain creates a disturbance in a river flow. The flow accelerates and separates at the upstream face of the abutment as it moves past the bridge abutment, creating a vortex trail that moves downstream in a direction approximately perpendicular to the structure. The result is that the bed erodes locally around the bridge abutment creating local scour hole [1]. There are approximately 600,000 bridges in the United States and 500,000 of them are over water [2]. During the last 30 years, more than 1,000 bridges have failed and 60% of those failures are due to scour, with earthquakes accounting for only 2% [3, 4]. Melville [5] reported that out of a total of 108 bridge failures recorded in New Zealand between the years of 1960 and 1984, 29 are related to abutment scour.

Excessive local scour at the bridge abutment may undermine the bridge foundation causing bridge failure [3]. Accurate prediction of the scour depth and pattern is essential for a safe and economic design of bridge foundation. Overestimation of the local scour leads to uneconomic design while underestimation of the local scour leads to unsafe design.

Although most of bridge failures are due to abutment scour, researches on pier scour received more attention. Flow field as well as resulting scour pattern around bridge abutments is still not well documented. Some scour prediction formulas are available in the literature to estimate the equilibrium scour at bridge abutments [1, 5-14].

Clear water abutment scour occurs in the absence of sediment transport by the flow into the scour hole from upstream. The clear water scour condition occurs when the velocity of the flow is less than the critical velocity of sediment transport ($V<V_c$). As the size of the scour hole increases, the local flow around the abutment is modified and the rate of scour is reduced until the equilibrium condition is reached where the maximum scour is attained [15].

When the flow approaches the abutment, the streamlines contract causing the flow to accelerate and consequently the local shear stresses increases by several orders of magnitude. At the upstream corner of the abutment, the turbulent shear stress is greater than the critical shear stress for the bed material causing initiation of motion. After initiation of scour and flow separation at the upstream side of the abutment, the flow is pushed to the downward direction into a strong spiraling flow causing the primary vortex to develop. As the strength of the primary vortex and downward flow increase, more sediment particles are eroded and removed from the scour hole causing the size and depth of the scour hole to increase. The scour hole continues to deepen and enlarge until equilibrium condition is reached. The scour hole around bridge abutment is said to be in equilibrium if the flow field

Corresponding Author: M.M. Abou-Seida, Irrigation and Hydraulics Department, Faculty of Engineering, Cairo University, Giza, Egypt.

and bottom shear stress inside the scour hole are no longer capable of moving sediments. In equilibrium condition, there is no change in the scour pattern with time. This definition is slightly different in the case of live bed scour as the scour pattern may vary with time due to the continuous movement of bed forms through the scour hole. In general, the scour hole shape is an inverted cone with some features of secondary groove due to the secondary vortices. A longitudinal ridge separates primary scour hole from this secondary groove [15].

The aim of the current study is to investigate the flow field around the vertical bridge abutment and the resulting scour pattern around the abutment formed in medium size non-cohesive sandy soil under clear water scour conditions. Also to develop a set of empirical formulas to predict equilibrium scour pattern around the bridge abutment (equilibrium scour depth, equilibrium scour width) in terms of the dominating factors that affect and control the scour process for sandy soils (Froude number, properties of erodible medium, and dimensions of the vertical-wall abutments).

MATERIALS AND METHODS

The experiments are performed in a horizontal flume 7 m long, 1 m wide and 0.5 m deep as shown in Figure 1. Two pumps are used to circulate the water through the flume. The first pump can circulate a flow ranging from 0.001 to 0.050 m^3/s, and the second pump can circulate a flow ranging from 0.001 to 0.030 m3/s. Both pumps can feed the flume separately or together. The flow goes through intake gravel tank and screen to reduce the turbulent eddies at the flume entrance. A wooden floating plate is used to absorb the surface waves. The testing section is about 1.40 m long. Then, water goes into collecting tank which connected with underground storage. Underground storage supplies water to both pumps. A calibrated flowmeter, fitted at the inlet pipe of the flume, is used to measure the flow discharge. The flow depth in the flume is adjusted by a downstream tailgate. A point gauge with an accuracy of ±0.1 mm is used to measure the flow depths. The point gauge is installed on a manually operated carriage running along the flume and it can also be moved along the carriage in the flume cross direction in order to reach any measuring point through the flume.

Three sizes of steel vertical-wall abutment are used with protrusion lengths perpendicular to the flow direction are 7.5 cm, 10 cm, and 15 cm. The abutment lengths in the flow direction are 15 cm, 20 cm, and 30 cm respectively. The three abutments have similar ratio of abutment length to protrusion length. Figure 2 shows a plan of flume and abutments dimensions and location of lateral and longitudinal profiles of the abutment scour hole.

Twenty four experiments for clear water scour conditions are performed with sandy soil as eroding bottom. The experiments are conducted with flow depth ranging from 10 cm to 14 cm and changing the discharge range to achieve the clear water scour range. Froude number ranges from 0.087 to 0.257.

Medium sand is used with median size D_{50} = 0.38 mm, Coefficient of Uniformity (C_u) = 2.74, Coefficient Curvature (C_c) = 1.03, and Standard Deviation = 1.7. The sand soil is sieved through sieve No. 4 in order to obtain the uniform size soil and to achieve the homogeneous distribution of water content throughout the soil. The sand is dumped around the abutment model in the sediment indention in the flume bottom under its own weight. Then the bed surface around the abutment is leveled by rectangular aluminum tube.

At the beginning of the experiment, the flume is filled with water very slowly from upstream and downstream sides. Then, the scour experiment starts with the required flow depth and flow rate. Each experiment is continued until approximately the equilibrium scour hole is fully developed and stabilized (attaining the equilibrium scour condition) or at least 90% of the equilibrium scour condition is achieved. The equilibrium condition of scour is defined as when the change of the maximum scour depth is 1 mm or less over 24 hours period of time. After equilibrium condition is reached and scour pattern stabilized, the scour hole is profiled in lateral and longitudinal directions to determine the geometry of the scour hole with a point gauge. The final bed elevations around the abutments are measured. These final bed elevations measurements are compared with the initial measurements to determine the shape or the scour hole and the maximum scour depth.

Detailed three-dimensional velocity measurements are performed for only three scour experiments which shown in Table 1. The detailed three dimensional velocity measurements are performed using Acoustic Doppler Velocimeter ADV. The results of the current scour experiments performed as part of this research are shown in Table 2. Figure 3 shows a schematic diagram showing the sign convention and abutment location within the flow field.

RESULTS AND DISCUSSION

The scour experiments of the present study are preformed using the medium sand of D_{50}=0.38mm as an erodible bottom. The variables which are allowed to change in the scour experiments are the flow velocity and the water depth. This arrangement make the Froude number a good dimensionless indicator of the

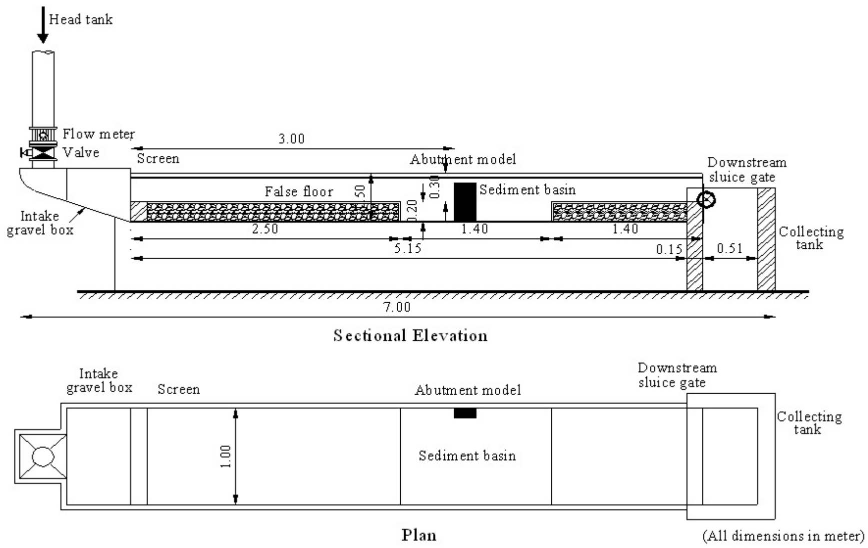

Fig. 1: Schematic layout of the experimental setup

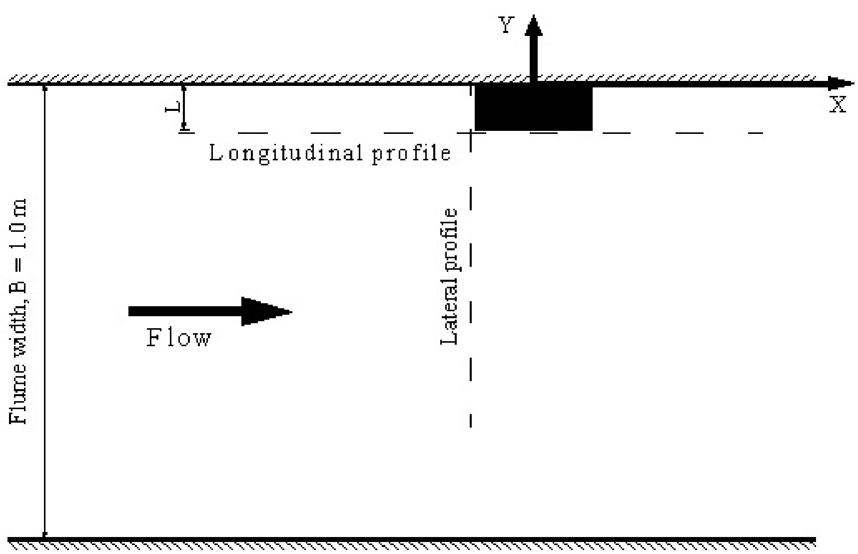

Fig. 2: Plan of flume and abutments dimensions and location of lateral and longitudinal profiles of the abutment scour hole

Table 1: Summery of the equilibrium experiments in sandy soil

Run ID	Abutment protrusion length (cm)	Discharge (m^3/s)	Flow depth (m)	Approach velocity (m/s)	Approach Froude number	Scour depth after 12 hr d_s (m)	Equilibrium scour depth after 84 hr d_{se} (m)	d_s /d_{se}
MS-7.5-5	7.5	0.0292	0.120	0.243	0.207	0.115	0.127	0.91
MS-10-15	10	0.0268	0.122	0.220	0.184	0.115	0.132	0.87
MS-15-21	15	0.0229	0.121	0.189	0.159	0.098	0.119	0.82

flow condition. The present study aims at the investigation of equilibrium scour pattern (scour depth, geometry, lateral profile, lateral side slope and longitudinal slope of the scour hole) as a function of Froude number and vertical-wall abutments dimensions.

Scour experiment are continued until the scour reaches equilibrium (change of the maximum scour depth is 1 mm or less over 24 hours period of time). Detailed three-dimensional velocity measurements are performed for only three scour experiments shown in Table 1.

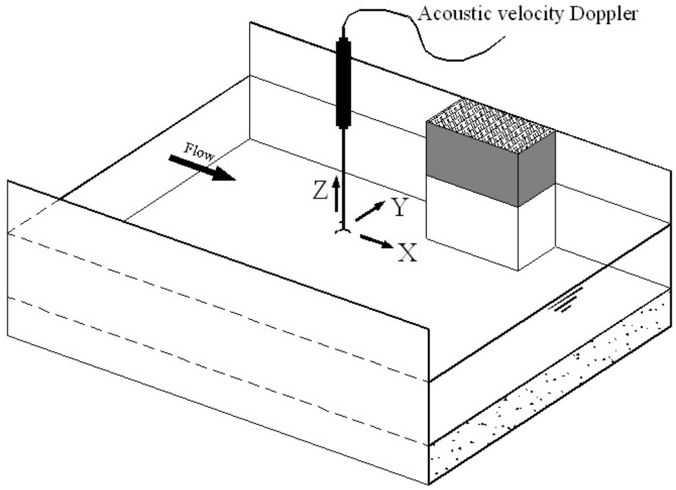

Fig. 3: Schematic diagrams showing the sign convention and abutment location within the flow field

Table 2: Results of sandy soil experiments

Run ID	Discharge (m^3/s)	Abutment protrusion length (m)	Water depth (m)	Approach velocity (m/s)	Approach Froude number	Scour depth after 12 hr (m)	Equilibrium scour depth (m)
MS-7.5-1	0.0131	0.075	0.120	0.109	0.093	0.016	0.024
MS-7.5-2	0.0168	0.075	0.120	0.140	0.119	0.031	0.042
MS-7.5-3	0.0218	0.075	0.120	0.182	0.154	0.057	0.070
MS-7.5-4	0.0250	0.075	0.119	0.210	0.180	0.068	0.079
MS-7.5-5	0.0292	0.075	0.120	0.243	0.207	0.115	0.127
MS-7.5-6	0.0354	0.075	0.120	0.295	0.251	0.170	0.175
MS-10-7	0.0126	0.100	0.115	0.110	0.097	0.033	0.048
MS-10-8	0.0167	0.100	0.119	0.140	0.120	0.040	0.054
MS-10-9	0.0183	0.100	0.120	0.152	0.129	0.053	0.069
MS-10-10	0.0189	0.100	0.119	0.159	0.136	0.056	0.072
MS-10-11	0.0211	0.100	0.120	0.176	0.149	0.064	0.079
MS-10-12	0.0231	0.100	0.122	0.190	0.158	0.070	0.085
MS-10-13	0.0240	0.100	0.119	0.202	0.173	0.100	0.118
MS-10-14	0.0252	0.100	0.121	0.208	0.175	0.111	0.130
MS-10-15	0.0268	0.100	0.122	0.220	0.184	0.115	0.132
MS-10-16	0.0290	0.100	0.121	0.240	0.202	0.125	0.139
MS-10-17	0.0304	0.100	0.115	0.264	0.234	0.162	0.171
MS-10-18	0.0356	0.100	0.119	0.300	0.257	0.192	0.196
MS-15-19	0.0131	0.150	0.124	0.106	0.087	0.040	0.061

Table 2: Continue

MS-15-20	0.0188	0.150	0.118	0.159	0.137	0.070	0.090
MS-15-21	0.0229	0.150	0.121	0.189	0.159	0.098	0.119
MS-15-22	0.0251	0.150	0.121	0.207	0.175	0.122	0.143
MS-15-23	0.0309	0.150	0.119	0.260	0.223	0.172	0.185
MS-15-24	0.0354	0.150	0.120	0.295	0.251	0.198	0.203

The detailed three-dimensional velocity measurements are performed using Acoustic Doppler Velocimeter ADV. The results of the current scour experiments performed as part of this research are shown in Table 2. In the experiments in which equilibrium scour was not attained, a least squares approach is utilized to estimate equilibrium scour depth d_{se} knowing the scour depth d_s.

$$\frac{d_s}{d_{se}} = 1.6156\ (F_r)^{0.3662} \qquad R^2 = 0.997 \tag{1}$$

Equilibrium Scour Depth: In the scour experiments, the Froude number ranges from 0.087 to 0.257 presenting the range of the clear water scour process. Figure 4 relates the dimensionless equilibrium scour depth to the Froude number of the flow. As shown in Figure 4 for all abutment protrusion length, the equilibrium scour depth and width increase as Froude number increases.

Scour Holes Geometry: Figures 5 through 7 shows the equilibrium scour pattern for sand scour experiments MS-7.5-5, MS-10-15, and MS-15-21 respectively. The scour pattern is similar for all the experiments. The scour hole at the upstream nose of the vertical wall abutment has the shape of partial inverted cone. The deepest point of the scour hole is located at the upstream nose of the abutment that make the slope of the scour hole is high at the upstream face of the abutment. This slope decreases gradually in the downstream direction and flatten out near the downstream end of the abutment. The scour hole features a secondary groove due to the secondary vortex. A longitudinal ridge separates primary scour hole from this secondary groove. The horizontal extents of the scour hole in the X- and Y-directions increase as Froude number increases. The sediment particles that erode and removed from the scour hole deposit at the downstream side of the abutment.

Lateral and Longitudinal Profile of the Scour Holes: Comparison of different lateral profiles passing through the upstream face of the abutment is conducted to study the effect of Froude number on the geometry of the scour hole. The locations of lateral and longitudinal profiles are illustrated in Figure 2.

Comparison of lateral profiles is illustrated in Figures 8, 9, and 10 for abutment protrusion lengths of 7.5 cm, 10 cm, and 15 cm for scour experiments MS-7.5-5, MS-10-15, and MS-15-21 respectively. The geometry of the scour is defined by the depth, width, and transverse side slope corresponding to equilibrium scour conditions. The equilibrium scour depth and width increase as Froude number increases. For all abutment protrusion length, the transverse side slope of the scour hole is approximately 29° (which close to the repose angle of medium sand used in the present experiments). Kwan [15] found this side slope to be approximately 26°. Changing of the flow Froude number and the abutment protrusion length do not have significant effect on the lateral side slope.

The equilibrium scour depth increases by 7.3 times as the flow Froude number increases from 0.093 to o.251 for abutment protrusion length = 7.5 cm (Figure 8). The equilibrium scour depth increases by 4.1 times as the flow Froude number increases from 0.097 to o.257 for abutment protrusion length = 10 cm (Figure 9). The equilibrium scour depth increases by 3.3 times as the flow Froude number increases from 0.087 to o.251 for Abutment protrusion length = 15 cm (Figure 10). It can be concluded that, the effect of changing the flow Froude number on the equilibrium scour depth is more pronounced for smaller abutment dimensions.

Scour Predictors for Sand Abutment Scour: Using the fitting techniques and the least squares approach, the following equations are developed from the results of the current scour experiments to estimate the abutment scour pattern in sandy soils. The following parameters are defined in the equations: d_{se} is equilibrium abutment scour depth in sandy soil, y is the average upstream flow depth, L is the abutment protrusion length, F_r is the Froude number of the upstream flow, and w_{se} is the equilibrium scour width.

Equilibrium scour depth: The equilibrium scour depth d_{se} can be estimated using equation (2).

$$\frac{d_{se}}{\sqrt{L\,y}} = 15.777\ (F_r)^{1.5943} \qquad R^2 = 0.926 \tag{2}$$

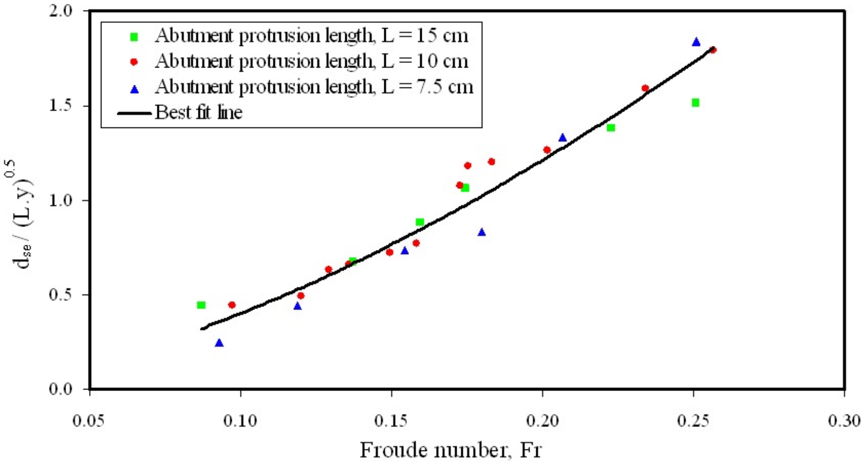

Fig. 4: Variation of dimensionless abutment scour depth with Froude number

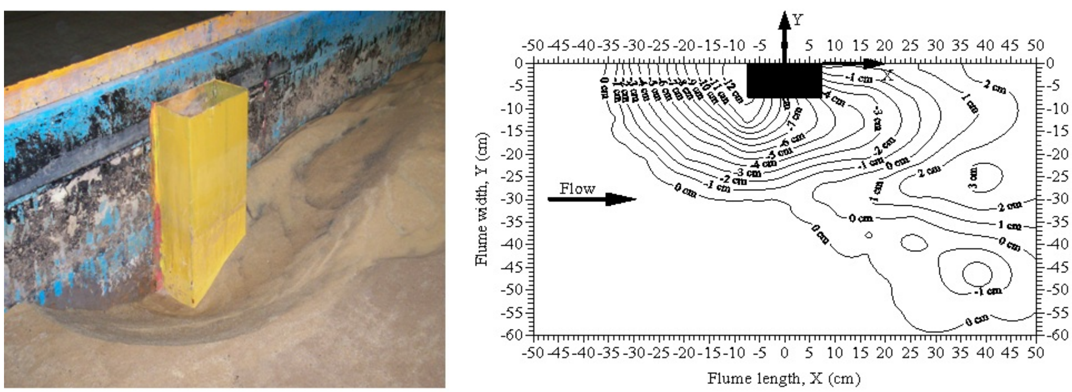

Fig. 5: Equilibrium scour pattern of experiment MS-7.5-5

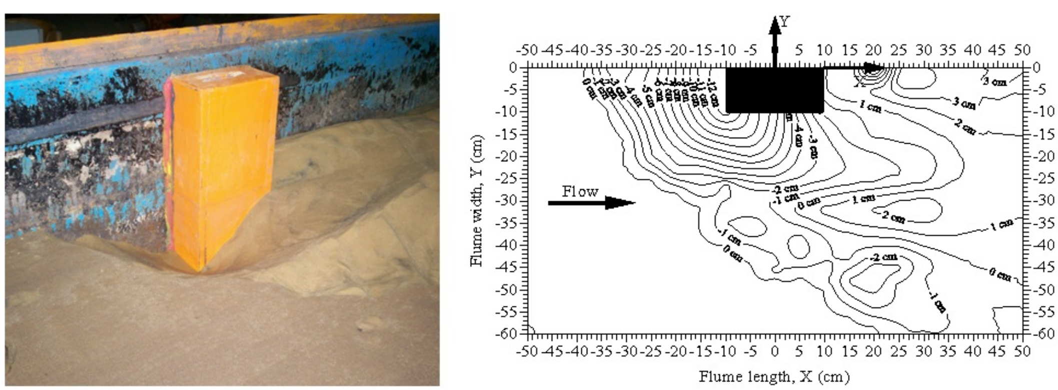

Fig. 6: Equilibrium scour pattern of experiment MS-10-15

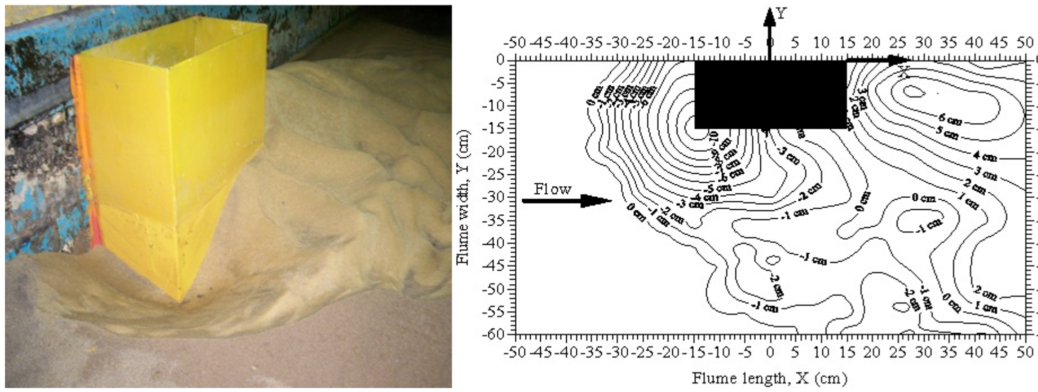

Fig. 7: Equilibrium scour pattern of experiment MS-15-21

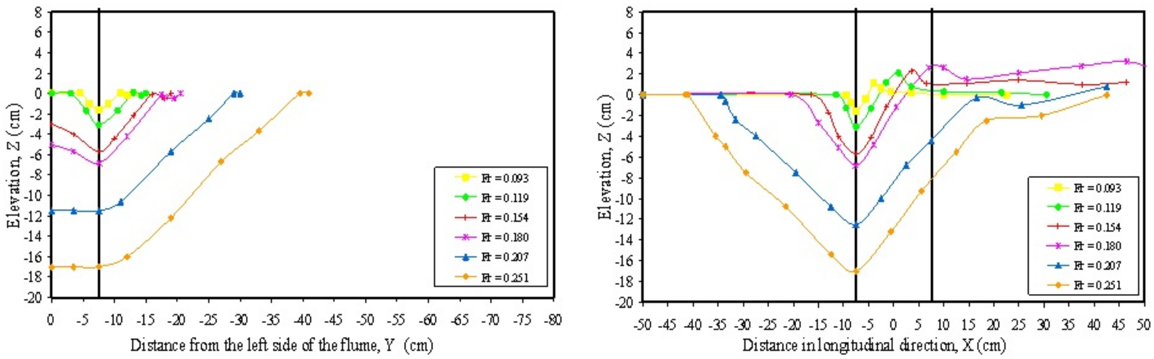

Fig. 8: Lateral and longitudinal profiles of the scour hole (Abutment protrusion length = 7.5 cm)

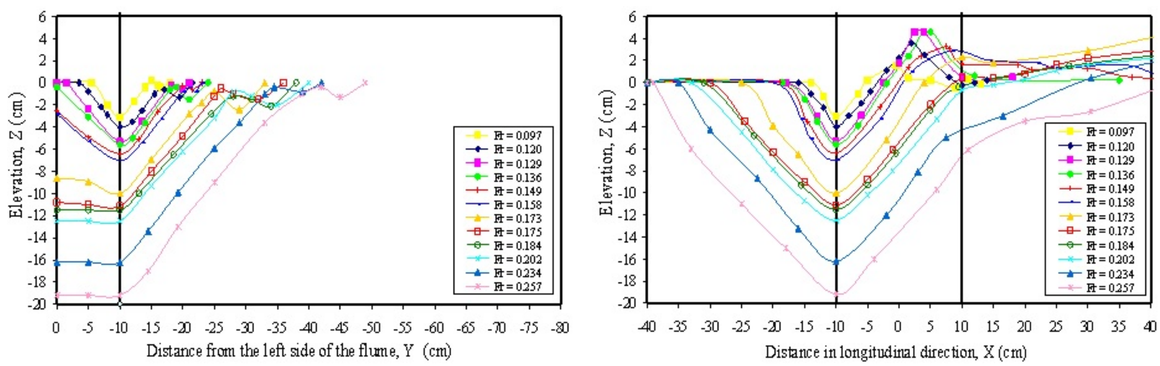

Fig. 9: Lateral and longitudinal profiles of the scour hole (Abutment protrusion length = 10.0 cm)

Equilibrium Scour Width: The equilibrium scour width w_{se} can be estimated using equation (3).

$$w_{se} = 1.804 \ d_{se} \qquad R^2 = 0.959 \tag{3}$$

Comparison of Present Study with Previous Studies for Sandy Soil: Figure 11 shows that, 91.7% of the measured results of the present study are within ± 20% limit lines of the computed data from the equation (2). The derived equation in the present study to estimate equilibrium scour depth d_{se} gives good reasonable prediction of d_{se}.

Figure 12 shows comparison of the equilibrium scour depth computed using equation (2) developed in the present study with abutment scour predictors available in literature. Equilibrium scour depth computed using the present study equation (2) is similar to Froehlich [11]. Equilibrium scour depths computed using equation (2) are greater than those estimated using scour predictor of Liu [9] and those

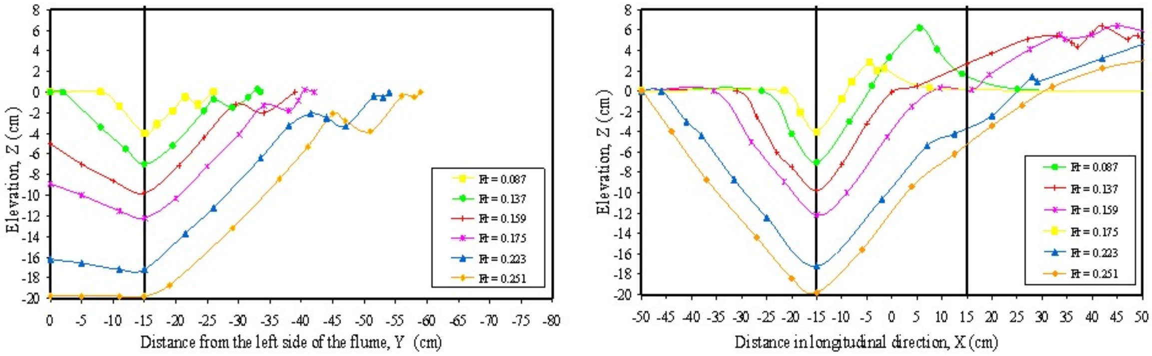

Fig. 10: Lateral and longitudinal profiles of the scour hole (Abutment protrusion length = 15.0 cm)

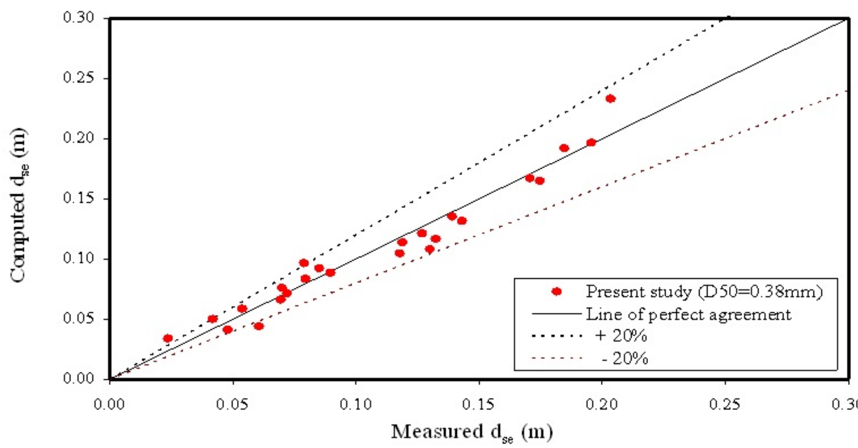

Fig. 11: Comparison of equilibrium scour depth computed using derived equation with measured data

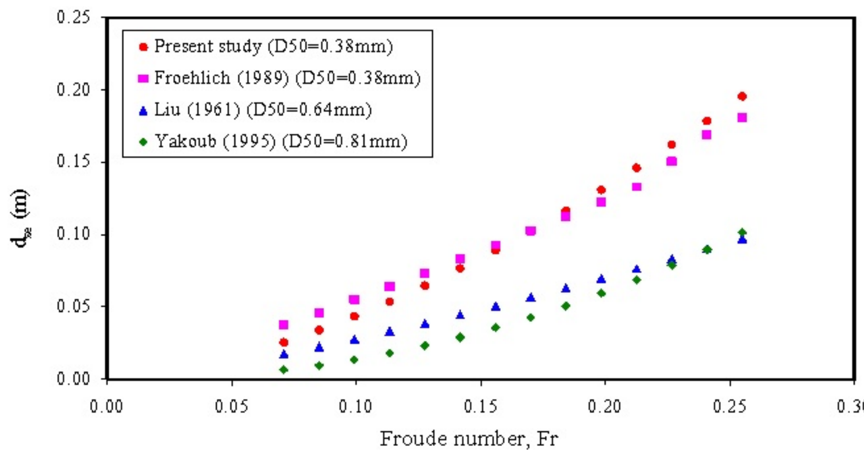

Fig. 12: Comparison of equilibrium scour depth computed using present study with previous study

estimated using the scour predictor of Yakoub [16] for the same conditions because the equations of Liu and Yakoub derived for sandy soil with D_{50} smaller than present study. Therefore, the derived equation (2) gives reasonable prediction of equilibrium scour depth.

From previous results, generally, it can be concluded the following:

Froude number and vertical-wall abutments dimensions are major factors in studying equilibrium scour pattern for sandy soil.

Equilibrium scour depth is directly proportional with Froude number and protrusion length of the vertical-wall abutments.

Equilibrium scour width is 1.8 equilibrium scour depth.

Practical formulas are developed to predict equilibrium scour pattern around the bridge abutment in terms of the dominating factors (Froude number and protrusion length of the vertical-wall abutments).

REFERENCES

1. Lim, S.Y., 1997. Equilibrium Clear Water Scour around an Abutment. Journal of Hydraulic Engineering, ASCE, 123(3): 237-243.
2. National Bridge Inventory, 1997. Bridge management Branch. Federal Highway Administration, Washington, D.C.
3. Briaud, J., F. Ting, H.C. Chen, R. Gudavilli, K. Kwak, B. Philogene, S. Han, S. Perugu, G. Wei, P. Nurtjahyo, Y. Cao and Y. Li, 1999. SRICOS: Prediction of Scour Rate at Bridge Piers. Texas Transportation Institute, The Texas A&M University, College Station, Texas, USA. Report, 2937-1.
4. Shirole, A.M. and R.C. Holt, 1991. Planning for a comprehensive bridge safety assurance program. Transp. Res. Rec. No. 1290, Transportation Research Board, Washington, D.C., 137-14.
5. Melville, B.W., 1992. Local Scour at Bridge Abutments. Journal of Hydraulic Engineering, ASCE, 118(4): 615-631.
6. Ahmed, M., 1953. Experiments on Design and Behavior of Spur Dikes. Proc. Int. Hydr. Convention, Univ. of Minnesota, Minneapolis, Minn., 145-159.
7. Laursen, E.M. and A. Toch, 1956. Scour around Bridge Piers and Abutments. Bull. No. 4, Iowa Highway Research Board, Ames, Iowa.
8. Garde, R.J., K. Subramanya and K.D. Nambudaripad, 1961. Study of scour around spur dikes. J. Hydr. Div., ASCE, 87(6): 23-27.
9. Liu, M.K., F.M. Chang and M.M. Skinner, 1961. Effect of Bridge Construction On Scour and Backwater. Deparment of Civil Engineering, Colorado State Universty, Report No. CER60-HKL22, February.
10. Gill, F.W., 1971. Flood Protection at Highway Bridge Openings. University of Newcastle, NSW, Engineering Bulletin CE3.
11. Froehlich, D.C., 1989. Abutment Scour Predication. Paper Presented at 68th TRB Annual Meeting, Washington, D.C.
12. Melville, B.W., 1995. Bridge Abutment Scour in Compound Channels. Journal of Hydraulic Engineering, ASCE, 121(12): 863-868.
13. Melville, B.W., 1997. Pier and Abutment Scour: Integrated Approach. Journal of Hydraulic Engineering, ASCE, 123(2): 125-136.
14. Molinas, A., 2004. Bridge scour in nonuniform sediment mixtures and in cohesive materials. Washington, DC, Federal Highway Administration Research Report FHWA–RD–03–083.
15. Kwan, T.F., 1984. Study of abutment scour. Rep. No. 328, School of Engrg., The Univ. of Auckland, New Zealand.
16. Yakoub, N.G.R., 1995. Effect of Cohesion on Bridge Abutment Scour. Ph.D. Thesis, Civil Engineering Department, Colorado State University, Fort Collins, Colorado, USA.